Interdependence between Structural Engineering and Construction Management
Edited by Ozevin, D., Ataei, H., Modares, M., Gurgun, A., Yazdani, S., and Singh, A.
Copyright © 2019 ISEC Press
ISBN: 978-0-9960437-6-2

FATIGUE LIFE ANALYSIS OF RAIL-WELDS USING LINEAR ELASTIC FRACTURE MECHANICS

MEQUANENT M. ALAMNIE[1] and YALELET ENDALEMAW[2]

[1]*Department of Engineering Science, University of Agder, Grimstad, Norway*
[2]*College of Engineering and Technology, Wolkite University, Wolkite, Ethiopia*

The initiation and growth of fatigue cracking is mainly due to high stress concentration, heterogeneity and poor quality of weld. The detection and rectification of such weld defects are major concerns of rail network managers to reduce potential risk of rail breaks and derailments. To estimate the fatigue life of welded joints and to analyze the progress of fatigue cracks, a fracture mechanics-based analysis and fatigue models were developed using Finite Element Analysis. The initial flaw is obtained from a sample weld using ultrasonic flaw detecting machine test. Linear Elastic Fracture Mechanics (LEFM) approach based on the Paris law was applied to determine critical crack size and the number of cycles to failure using FRANC3D software. The inspection interval of rail welds before fracture (failure) was suggested based on reliability and life cycle analysis that correspond with minimum overall cost and frequency interval. It is recommended that fracture-based models in combination with reliability analyses can be a sustainable infrastructure decision-making algorithm.

Keywords: Ultrasonic test, Paris law, FRANC3D, Inspection interval.

1 INTRODUCTION

Railway infrastructures are high investment assets. They are designed to work in a very demanding safety conditions and must display a very low occurrence of failures. Rails are the most significant and basic components of railway systems. However, different factors, which influence the rail degradation process gradually reduce the performance, reliability and safety of railway infrastructure. Railway rails are manufactured in sections of 25 - 120 m length, which are joined in track by either bolting or welding. The joints and track irregularities are the weak sections associated with high risk of failure (Ringsberg *et al.* 2005). The service performance of rail-welds is affected by their ability to support the service load without fatigue damage. Fatigue and fracture behavior are important considerations in determining the condition of metal structures subjected to cyclic loads. Specifically, the expected life of a rail-weld subjected to random, variable-amplitude traffic cycles are highly dependent upon damage accumulation caused by various fatigue mechanisms. Structural failure is seldom attributed to load considerations; the occurrence of stresses exceeding those predicted by the designer is rare (Peter and Thomas 2011). This paper is aimed at determining the response of rail-welds to fatigue load using linear fracture mechanics approach. A Cost model is also employed to address the trade-offs among various factors related to rail defect and inspection frequency (Sauragh 2008).

2 RAIL WELDING

According to the American Society of Welding, welding is a localized coalescence of metal where coalescence is produced by heating to suitable temperature, with or without the use of filler metal. Alumino-thermic (thermite) welding is a process that produces coalescence of metals by heating them with a powdery mixture of metallic aluminum (Al~22%) and iron scale (Fe_3O_4~78%) as a thermite (Sergejevs and Mikhaylovs 2008, Napoleon 1997, Ringsberg *et al.* 2005). Weld sample used in this paper is a thermite weld. Visual examination of the weld for visible defects by the welding personnel such as geometry is first test. *Ultrasonic, Hardness, Slow Bends Test, Fracture Surface Examination, and Micro-and Macro Structure Examination* are other tests for weld quality (Liu *et al.* 2014). Ultrasonic Testing (UT) uses high frequency sound waves (typically 0.5 and 15 MHz) to conduct examinations and make measurements. It has wide use in engineering applications (*flaw detection/evaluation, dimensional measurements, material characterization, etc.*). A typical pulse-echo UT inspection system consists of several functional units, such as the pulser/receiver, transducer, and a display device. Angle beam transducers and wedges are typically used to introduce a refracted shear wave into the test material. An angled sound path allows the sound beam to come in from the side to improve detectability of flaws in weld areas.

3 FRACTURE MECHANICS

Fracture mechanics is broadly classified into two types: Linear Elastic Fracture Mechanics (LEFM) and Elastic Plastic Fracture Mechanics (EPFM). LEFM assumes small deformation and minimal yielding at the crack tip, while EPFM can account large deformation and plastic effects. In LEFM, stress intensity factor (SIF) is a measure of the stress field at the crack tip. In general, the stress intensity factor is proportional to the remote stress σ, crack size a, and the geometry of the mechanical component with crack and serve as a measure of the severity of the crack tip for different crack configurations. Paris's law (Eq. (1)) is used for fatigue crack growth analysis (Paris and Erdogan 1963).

$$\frac{da}{dN} = C(\Delta K(a))^m \tag{1}$$

Where C and m are material parameters in Paris region (3 and $1*10^{-11}$ respectively) (David 2001), $\Delta K = K_{max} - K_{min} = \Delta\sigma\sqrt{\pi a}$, K_{max} (maximum) and K_{min} (minimum) stress intensity factors.

The number of cycles to failure, N_f, can be obtained by integrating (Eq. (1)) with respect to crack size a, from initial crack size, a_i, to final crack size, a_f, as indicated in Eq. (2) and Eq. (3).

$$N_f = \int_{a_i}^{a_f} \frac{da}{c[\Delta\sigma\sqrt{\pi a}]^m} \tag{2}$$

$$a_f = \frac{1}{\pi}\left[\frac{K_{IC}}{c[\Delta\sigma\sqrt{\pi a}]^m}\right]^2 \tag{3}$$

Where, K_{IC} is the fracture toughness.

3.1 Fracture Behavior of Rail-Welds

For thermite welds after crystalline rearrangement Poisson's ratio and modules of Elasticity are in the range of -17% to +13% and ∓5%, respectively (IACS 2016). Since the material at the running surface of the weld, and some millimeters beneath, is strongly deformed and compressional residual stresses are generated in that region, and since the global bending stresses are highest in the foot, fatigue cracks in the welded rails tend to grow from underneath rather than from the railhead (Zerbist *et al.* 1978).

3.2 Flaw Detection of Weld Sample

Flaws are detected on the rail weld at the rail base using a “crack tip diffraction” technique. An angled transducer of 60° and using the shear velocity of sound in steel as 3130mm/s are used so that, it could be used as a tip for discontinuity/flaw (Det Norske Veritas 2004). The flaw size can be determined as half the velocity of sound in the rail, 3130mm/s multiplied by the product of the time taken by the sound to traverse the flaw, which is 100 μsec and cosine of angle of transducer used in the determination (Figure 2a). Thus, the flaw size is shown in Eq. (4) as:

$$a = \frac{dtV}{2}\cos(\theta_R) = \frac{1}{2}(100\mu\text{sec}) * (3130\text{mm/s}) * \text{Cos }(60°) \cong 0.07825\text{mm} \tag{4}$$

3.3 Optimal Inspection Interval

Preventive replacement and periodical inspections are two major approaches used for improving system availability and reducing maintenance cost. The Association of American Railroads (AAR) developed a Rail Defect Detection Cost Model that estimates the total cost of repairing detected defects and broken rails (Orringer 1990). Based on a model developed by AAR, the long-term cost of Rail-welds is given by Eq. (5) (Liu *et al.* 2014).

$$K\frac{L}{V}C_{hr} + \frac{S(K)L}{h\left(\frac{T}{K}-q\right)}(DDC + C_{DDT}) + S(K)L(S_{DC} + C_{SDT}) \tag{5}$$

K is annual inspection interval; L is track length (mi); V is average inspection vehicle speed (mph); C_{hr} is inspection cost per hour per vehicle($/hr/veh); S(K) is annual number of broken rail per mile; h is parameter related to inspection frequency (≈ 0.0108); T is annual traffic density(MGT); DDC is cost of repairing detected weld defect($); C_{DDT} is train delay cost due to fixing a detected defect($); S_{DC} is cost of repairing broken rail($); C_{SDT} is train delay cost due to fixing a broken rail($).

4 WHEEL-RAIL CONTACT STRESS ANALYSIS

The forces arising between wheel and rail contact generate contact stresses in a local volume of the two bodies. Hertzian-Contact-Model describes the local stresses with good accuracy for the most common wheel-rail contact problems (Kalker 1991). The distribution of the contact pressure in this elliptical area represents a semi-ellipsoid, which can be expressed as Eq. (6):

$$P(x,y) = \sqrt{1 - \frac{x^2}{a^2} - \frac{y^2}{b^2}} \times \text{P}_\text{o} \tag{6}$$

Where, a and b are semi axes, and x and y are the required coordinates to specify the point of contacts on the rail surface based on the lateral rail surface parameter. The location of the contact point depends on the relative position of the wheelset with respect to the rail and the two bodies’ profile. If $x = 0$ and $y = 0$ that is if the point of contact is on the centerline of the railhead, the stress is maximum, which is equal to Eq. (7):

$$P(x,y) = P_o = \frac{3N}{2\pi ab} \tag{7}$$

The dynamic effect of static wheel load, $F_V^{\mathbf{dyn}}$ is modeled as a statistical distribution by multiplying the static load, N with a magnification factor (K_{dyn}) (Eq. (8) to (10)).

$$F_y^{dyn} = K_{dyn} \times N \tag{8}$$

$$K_{dyn} = 1 + 3n\varphi \tag{9}$$

$$\varphi = \begin{cases} 1 & \text{for } V \leq \frac{60Km}{hr} \\ 1 + \frac{0.5(V-60)}{190} & \text{for } 6o \leq V \leq \frac{300Km}{h} \text{ for Passenger train} \\ 1 + \frac{0.5(V-60)}{80} & \text{for } 60 \leq V \leq \frac{140Km}{h} \text{ for freight train} \end{cases} \tag{10}$$

Where n= 0.15 to 0.25 for different types of track, 0.2 for normal wheel-rail contact and φ is coefficient due to speed (Peter and Thomas 2011), V = train speed.

4.1 Finite Element Modelling

The track components, namely, the rail, the sleepers, the wheel, and the weld are modeled assigning their respective material properties and in their respective positions. Meshing the assembly of those parts as seen in Figure 1 (a and b), the job is submitted for analysis and is then exported to FRANC3D for further analysis (ABAQUS 6.12 1998), (FRANC3D 2011).

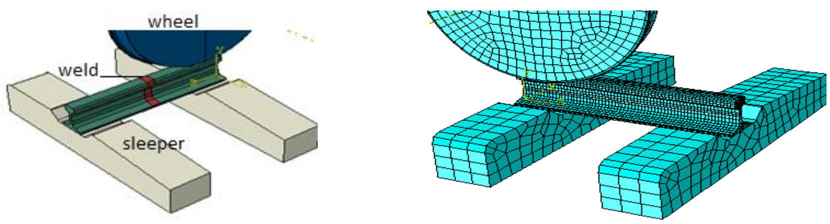

(a) (b)

Figure 1. ABAQUS FE Modeling of welded track.

5 RESULT AND DISCUSSIONS

5.1 Contact Stress Analysis

In rail welds, as the molten metal cools with crystalline re-arrangement, there is a wide variation in modules of elasticity and Poisson's ratio (IACS 2016). Two cases considered (maximum and minimum) Case 1; E_{max} and μ_{min} and Case 2; E_{min} and μ_{max} the response of these Weldments to contact stress is depicted for different train speed. The contact stress is verified from both empirical and FEA.

Table 1. Contact stress comparison of the Base and Welded rail with different crystalline rearrangement.

Speed (Km/hr.)	For base rail			For Weld (Case 2)			For Weld (Case 1)		
	a (mm)	b (mm)	P_o (N/mm^2)	a (mm)	b (mm)	P_o (N/mm^2)	a (mm)	b (mm)	P_o (N/mm^2)
60	8.983	6.747	1546.58	8.92	6.7	1566.73	9.0923	6.829	1509.49
70	9.052	6.799	1558.57	8.99	8.99	1185.86	9.1628	6.8819	1521.19
80	9.121	6.85	1570.38	9.06	6.8	1590.84	9.2322	6.9341	1532.72
90	9.188	6.901	1582.01	9.12	6.85	1602.63	9.2322	6.9341	1567.03
100	9.255	6.951	1593.48	9.19	6.9	1614.24	9.368	7.0361	1555.26
110	9.321	7.000	1604.78	9.26	6.95	1625.69	9.3206	7.0005	1604.78
120	9.385	7.049	1615.92	9.32	7.00	1636.98	9.4999	7.1352	1577.17

5.2 Fatigue Life Computation

FRANC3D is a program that inserts and extends a crack and/or voids in a pre-existing finite element meshes to see a fracture response of material. In this paper, the ABAQUS/CAE model is exported and the initial crack (0.07825mm) found from the UT is inserted and the model is re-meshed with the inserted crack as shown in Figure 2.

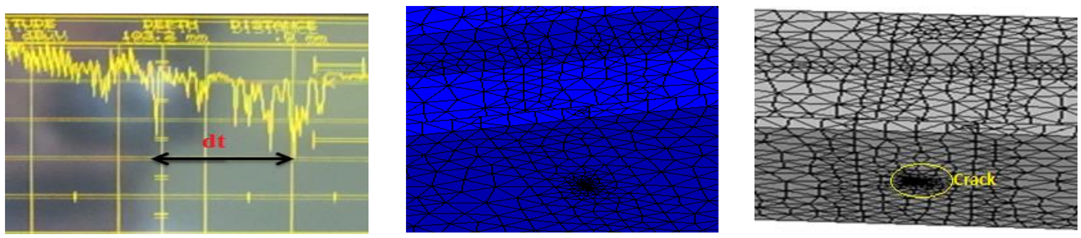

(a) (b) (c)

Figure 2. (a) Echograph of UT (b) and (c) Re-meshed Model with elliptical initial crack geometry.

The analysis of a fracture-based fatigue model in FRANC3D estimated the crack growth rate versus number of cycles to failure, and the maximum crack growth versus maximum stress intensity facture to fracture (See Figure 3 (a) and 3(b)). With different initial crack sizes, the response of weldment to remaining number of cycles to failure is determined.

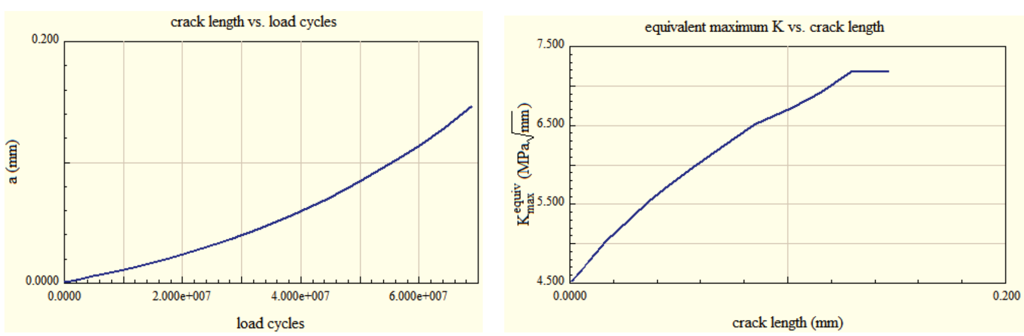

(a) (b)

Figure 3. *(a)* crack growth Vs. number of cycles *(b)* Crack length Vs. K_{max}.

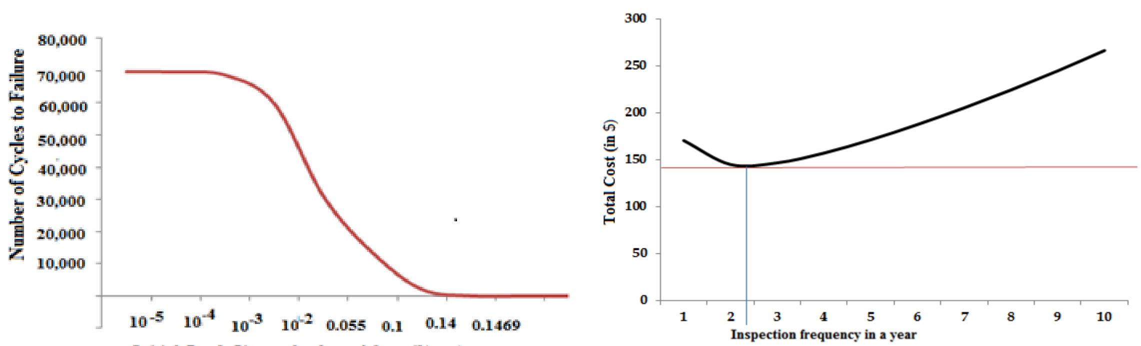

(a) (b)

Figure 4. (a) Load frequency and crack growth (b) Total cost ($) and annual inspection frequency.

5.3 Inspection Interval

Using a model developed by AAR (the cost items are modified based on case study data), the calculated total long-term cost is shown for different inspection frequencies.

As can be seen in Figure 4, the inspection interval which balances the cost of inspection from frequent inspection and failure cost from an infrequent inspection can be balanced at an inspection interval of at least two times a year or nearly every five-month interval.

6 CONCLUSIONS

In this paper, a fracture mechanics based approach was applied to analyze the performance of rail weld joint from Ethiopian railways project. After detecting a flaw in the thermite weld, a finite element method based on Paris law is develop to analyze the fatigue response of the weld subjected to 12.5 ton wheel load at different speed until the critical crack reached. Based on cost model, the inspection interval is estimated that corresponds to minimize the overall defect prevention cost. The remaining number of cycles to failure and fatigue crack growth rate is determined to decrease with a very small increment of an initial crack size.

In addition, as the material property of welds is slightly different from the base rail for a weld with a lower elastic modulus and higher Poisson's ratio (μ), the contact stress at the weldment exceeds the base rail. However, as the crystalline of the weld is rearranged in a manner with larger E and smaller μ the contact stress slightly lessen the contact stress between the base rail and the wheel. The result of this paper can be a starting point to develop a methodology for further detail repair and replacement of the rail, i.e., Maintenance strategy Models.

References

Abaqus 6.12, *Dassault System Center of Simulation Excellence,* Theory Manual, 1998.

David R., *Fatigue*, Department of Material Science and Engineering, MIT, Cambridge MA, 2001.

Det Norske Veritas, *Introduction to Non Destructive Testing Techniques*, Ultrasonic Testing, 2004.

Franc3D, *Fracture Analysis Consultant*, Inc., Reference Manual, 2011.

IACS, *Requirements Concerning Materials and Welding*, International Association of Classification Societies, 2016.

Kalker J., Wheel-Rail Rolling Contact Theory, *Wear*, 144, 243-261, 1991.

Liu, X., Dick, C. T., and Saat, M. R., *Optimizing Ultrasonic Rail Defect Inspection to Improve Transportation Safety and Efficiency*, The Second T&DI Congress in Orlando, FL, June 8-11, 2014.

Napoleon, *Railway Applications-Track Alumino-Thermic Welding of Rails*, OH, 1997.

Orringer, O., *Control of Rail Integrity by Self-Adaptive Scheduling of Rail Tests*, Federal Railroad Administration, Washington, D.C., 1990.

Paris, P., and Erdogan, F., A Critical Analysis of Crack Propagation Laws, *Journal of Basic Engineering*, 85(4), 528-533, 1963.

Peter J., and Thomas, T., *Fatigue Behavior of Steel Highway Bridge Detail*, Virginia, 2011.

Ringsberg, J. W., Josefson, B. L., and Skyttebol, A., *Fatigue Crack Growth in Welded Rails*, Göteborg, Sweden, 2005.

Sergejevs, D., and Mikhaylovs, S., Analysis of Factors Affecting Fractures of Rails Welded by Alumino-Thermic Welding, *Transport Problems*, 3(4), 33-37, 2008.

Sauragh, K., *Reliability Analysis and Cost Modeling of Degrading Systems*, Ph.D. Thesis, Division of Operation and Maintenance Engineering, Luliya University, 2008.

Zerbist. U., Lauden, R., Eden L., and Smith, R., *Introduction to the Damage Tolerance Behavior of Railway Rails*, Philadelphia, PA., 1978.